SIGRA™ PTY LTD
Professional Engineers
and Geoscientists
ABN 68 061 279 427
http://www.sigra.com.au

93 COLEBARD STREET WEST
ACACIA RIDGE
BRISBANE
QUEENSLAND 4110
AUSTRALIA

TEL: +61 (0)7 3216 6344
FAX: +61 (0)7 3216 6988
EMAIL: info@sigra.com.au

ROCK PROPERTY TESTING

Version:	1.0
Revision Date:	04/06/2020
Author(s):	X. Zhao J. Pham D. Smith I. Gray

FOREWORD

This document outlines some of the rock property test methods in use by Sigra Pty Ltd. It is designed to supply descriptions of the various tests in use and the information that can be derived from them. Theory of the test procedures is included where this has not been adequately documented elsewhere.

The testing methods described are being continually updated so attention should be paid to the date and version of this document.

Dr Ian Gray
Principal Engineer
Managing Director

TABLE OF CONTENTS

FOREWORD 1
TABLE OF CONTENTS 2
TABLE OF FIGURES 3
INTRODUCTION 4
Loading Cases for Various Tests – as shown in Figure 1. 4
SUMMARY AND USE OF TESTS 7
Simple Uniaxial Testing (UCS) 7
Uniaxial Testing with Strain Measurement (UCS, E_1, $\boldsymbol{V}_{12}$) 7
Cyclic Uniaxial Testing with Strain Measurement (UCS, $\boldsymbol{E1}$, $\boldsymbol{V}_{12}$, $\boldsymbol{\varepsilon p}$) 7
Simple Shear Testing (approximate cohesion) 7
GOST Shear (Mohr-Coulomb C and Phi) 7
Triaxial Failure (Mohr-Coulomb C and Phi) 8
Triaxial Elastic ($\boldsymbol{Ei}$, $\boldsymbol{Vij}$, $\boldsymbol{\alpha i}$) 8
Hydrostatic Testing ($\boldsymbol{Ei}$) 8
Transverse Tensile Testing 9
Axial Tensile Testing 9
Slake Testing 9
Point Load Strength Index Testing 9
Brazilian Test 10
Protodyakanov Index Test (f) 10
Other Tests 10
CYCLIC UNIAXIAL TESTING WITH STRAIN MEASUREMENT 11
Relationship between tangent and secant Young's moduli and Poisson's ratios from uniaxial testing 18
SIMPLE SHEAR TESTING 20
MODIFIED GOST (ГОСТ) SHEAR TESTING 21
TRIAXIAL FAILURE TEST 23
TRIAXIAL ELASTIC TESTING 24
HYDROSTATIC TESTING 27
TRANSVERSE TENSILE TESTING 28
AXIAL TENSILE TESTING 31
SLAKE TESTING 32
POINT LOAD STRENGTH INDEX TESTING 33
BRAZILIAN TEST 34
PROTODYAKANOV INDEX TEST (f) 35
References 37

TABLE OF FIGURES

Figure 1: Various test stress states plotted as Mohr's Circles and points on a plot of shear stress versus normal stress 6
Figure 2: Uniaxial test specimen fitted with axial and circumferential strain rosettes 11
Figure 3: Axial and circumferential strains versus time 12
Figure 4: Plot of axial and circumferential strains versus axial stress for a sandstone 12
Figure 5: Picks of load and strains from a uniaxial test – schematic 13
Figure 6: Residual strains following loading 14
Figure 7: Tangent loading Young's modulus calculated by data points 14
Figure 8: Endpoints of stress and strains from cyclic loading cases 15
Figure 9: Plots of Young's moduli versus stress derived from the same uniaxial test 16
Figure 10: Poisson's ratios calculated by various methods 17
Figure 11: Plot of axial and circumferential strains versus axial stress for a typical coal sample 18
Figure 12: Direct shear test on a core specimen 20
Figure 13: Core Shear Strength Testing Apparatus, Top view 20
Figure 14: Test sample after failure, Side View 20
Figure 15: Modified GOST Shear Test Apparatus 21
Figure 16: Modified GOST Shear Test Setup 22
Figure 17: View of failure surface. 22
Figure 18: Side view of sample before and after failure. 22
Figure 19: Modified GOST Shear Test Plot 23
Figure 20: Showing a fine grained silty sandstone core fitted with strain gauge rosettes within the triaxial cell prior to the sleeve being fitted. 24
Figure 21: Example of the first cycle of stepwise axial pressure (AP) and confining pressure (CP) in kPa changes and the resulting strains in microstrain. 25
Figure 22: Axial Young's modulus for a core of porous sandstone drilled perpendicular to the bedding. 26
Figure 23: Strain gauged phyllite sample cast in silicone resin. 27
Figure 24: Prepared sample disc 28
Figure 25: Prepared sample glued between two sets of steel plates. 29
Figure 26: Test sample before in UTM before failure 29
Figure 27: Failed transverse tensile test disc. 30
Figure 28: Example Plot of Microstrain vs Applied Stress 30
Figure 29: Example of Axial Tensile Test 31
Figure 30: Tensile test specimen before and after testing. 31
Figure 31: Assessment of Rock Behaviour 32
Figure 32: Point load test of an irregular specimen in the laboratory. 33
Figure 33: Site Brazilian test equipment – test cylinder with pressure pump 34
Figure 34: Test sample after failure – Side View 34
Figure 35: Drop hammer equipment – measuring cylinder with scale and tube with drop hammer. 35

INTRODUCTION

Sigra undertakes a range of rock property measurements. These produce information on rocks prior to reaching their peak strength and in terms of peak strength. In addition, the poroelasticity and plastic deformation are also determined in some test procedures. The test emphasis at Sigra is on measuring the important rock parameters for a given situation, not in simply producing multiple standard test results which are of little or no value.

Table 1 shows the rock testing that is undertaken by Sigra split into laboratory and field procedures. The table also shows the parameters that may be gained from each test. These are colour coded to show the quality of the parameter derived from each test. Those in blue are direct and high quality, those in green less so, while those in orange are derived from index tests and are arrived at by correlations rather than fundamental measurement.

Loading Cases for Various Tests – as shown in Figure 1.

Figure 1 shows some of the measurements presented on a Mohr's circle plot of shear stress versus normal stress and showing a Mohr-Coulomb failure envelope line.

The uniaxial tests are shown having the lower principal stress being zero while the major principal stress in the axis of the test loading is the uniaxial compressive strength.

The Sigra simple shear directly shears the sample and so it is centred on the origin of the plot.

The GOST shear test enables shear and normal load to be applied to failure. A failure point on the Mohr-Coulomb line for this test is shown.

Triaxial tests involve testing the sample to failure under axial load with confinement and so the major and minor stresses at failure are measured.

The tensile tests involve pulling the sample apart without any lateral loading and hence plot on the negative side of zero stress with one principal stress being zero.

The three index tests – Brazilian, Protodyakonov and Point Load – all involve loading the specimen of rock in compression. By a function of the geometry of the specimen and the point or line loading of the rock, a complex stress state that involves compression and tension occurs. Shear is therefore generated. Hence the Mohr's Circle shown for these tests is shown in green and is somewhat vague. The test results are however valuable in their own right.

The hydrostatic test does not lead to failure unless the sample is porous and crushes. It plots as a point in the Figure 1. This point progresses to the right as the hydrostatic stress increases.

It should be appreciated that rock fabric (bedding, foliation) and joints have a huge effect on the rock properties, and tests used need to reflect what is being measured. For example, it is of limited use measuring uniaxial compressive strength of a sample drilled normal to a foliation or bedding plane if failure is expected to occur by shear along the plane or by tensile failure across it.

Test Type	Axial modulus E1	Trans modulus E2	Trans modulus E3	Axial Poisson's Ratio V12	Geometric mean Poisson's Ratio Va	Poroelastic coefficients	Plastic defor mation	Uniaxial compressive strength	Axial tensile Strength	Transverse tensile strength	Cohesion C	Friction ϕ
Laboratory												
Simple Uniaxial												
Cyclic Uniaxial												
Simple shear												
GOST shear												
Triaxial - Elastic												
Triaxial - Failure												
Hydrostatic												
Transverse tensile												
Axial tensile												
Slake												
Field												
Point Load												
Brazilian												
Protodyakanov												

Table 1: Rock property testing undertaken by Sigra showing results that may be derived from the tests

E1 = Young's modulus in the axial direction of the core
E2 = Young's modulus (minor) perpendicular to the core
E3 = Young's modulus (major) perpendicular to the core
V12 = Poisson's ratio measured by axial loading of the core
C = Cohesion according to Mohr-Coulomb theory
ϕ = Friction angle according to Mohr-Coulomb theory
Va = Geometric mean Poisson's ratio

High quality measurement	
Second quality measurement	
Derived from index test	

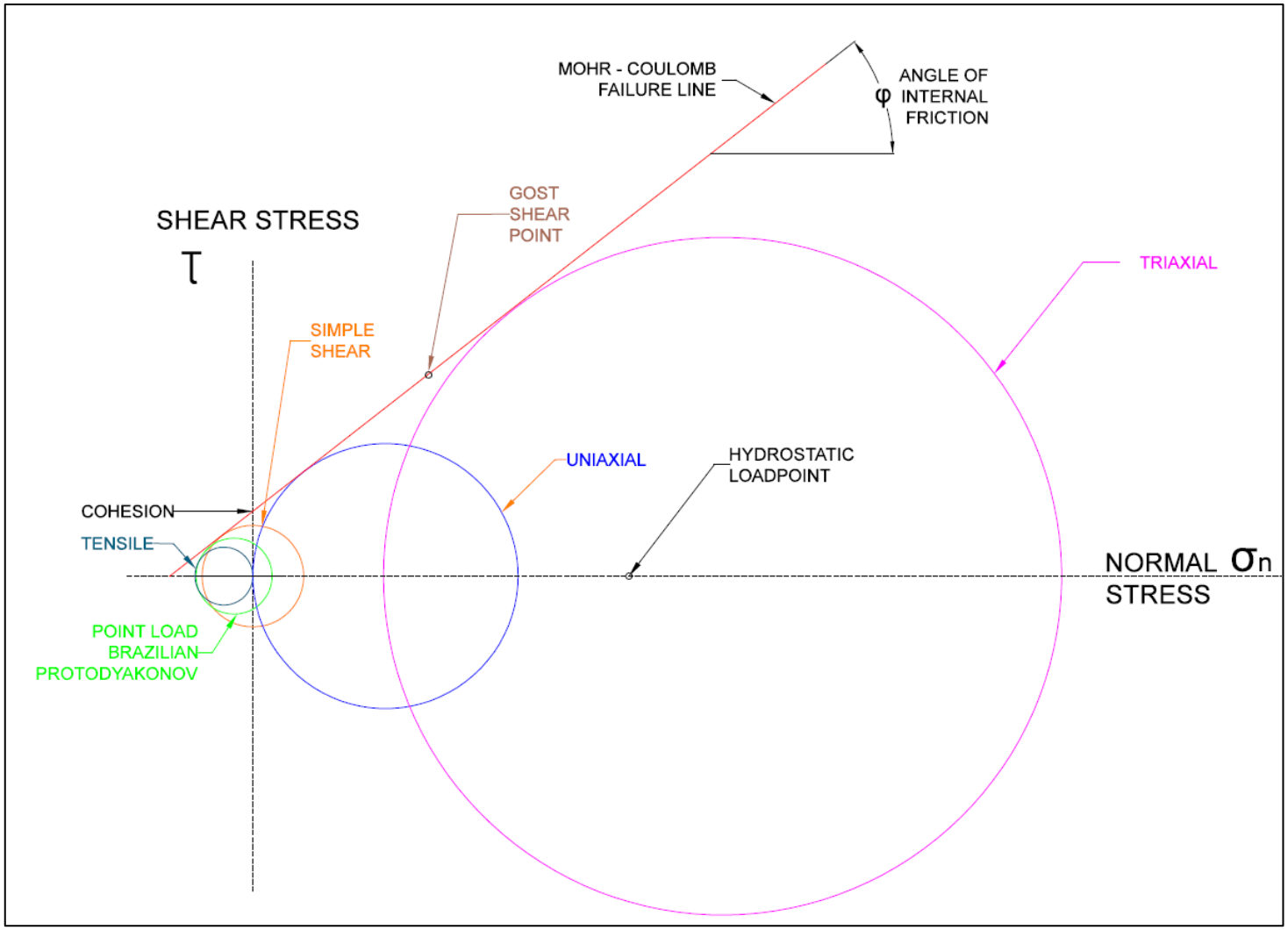

Figure 1: Various test stress states plotted as Mohr's Circles and points on a plot of shear stress versus normal stress

SUMMARY AND USE OF TESTS

Simple Uniaxial Testing (UCS)

This involves loading a core sample uniaxially along the core axis in a single loading cycle to failure. The peak load at failure is recorded and converted to a Uniaxial Compressive Strength at failure (UCS) in units of stress. This is a basic measurement that is frequently used as an indication of rock strength. The values of strength derived are highly dependent on the orientation of the sample with respect to rock fabric.

Uniaxial Testing with Strain Measurement (UCS, E_1, V_{12})

This involves loading a core under axial load while monitoring its axial and circumferential deformation either by strain gauges or LVDT systems. The test enables the measurement of Axial Young's modulus (E_1) and Poisson's ratio (V_{12}) associated with axial load alone. This value of Poisson's ratio tends to be high, as it is influenced at higher stresses by high near surface deformation. The test is usually taken to failure and a UCS value derived.

Cyclic Uniaxial Testing with Strain Measurement (UCS, E_1, V_{12}, ε_p)

This involves loading an instrumented core axially under cyclic loading conditions. In each cycle the core is loaded and unloaded. The results are separated into elastic and plastic deformation measurements. Axial Young's modulus (E_1) and Poisson's ratio (V_{12}) are derived from the test on an elastic basis. The plastic axial and circumferential deformation (ε_{pa} and ε_{pc}) at the end of each loading cycle is also presented in terms of axial stress versus axial and circumferential strain.

Simple Shear Testing (approximate cohesion)

This test is designed to test the shear strength of laminated core. It is particularly suited to sedimentary rocks with a weak bedding plane that is perpendicular to the core. The test involves sitting the core in a saddle and loading centrally so that each end of the core is subject to an equal shear stress. The core almost invariably breaks at one end as one end will be weaker than the other. The value of shear stress at failure is calculated as half the load divided by the cross-sectional area of the core.

GOST Shear (Mohr-Coulomb C and Phi)

This test is derived from the Russian standard ГОСТ 21153.5-88. It involves inserting a core into a split cavity on each side of a split cylinder. The split cylinder is then rotated to a test angle and is loaded to failure. The loading applies normal stress and shear to the plane of the core between the split cylinder and shears the rock. By shearing sequential specimens at different angles, a variety of values of shear and normal stress at failure are acquired. These may be presented on a plot of shear stress versus normal load, and the cohesion and angle of internal friction can be derived. The original standard shows the core being sheared longitudinally. In the Sigra version the core is sheared transversely. In this mode the shear strength behaviour of bedding planes is directly measured. The test apparatus can accommodate specimens that are from 30 to 60 mm long. This enables a number of test samples to be obtained from a short length of core.

Triaxial Failure (Mohr-Coulomb C and Phi)

This test involves the use of a Hoek cell to determine failure of a core under axial load with confining stress supplied by hydraulic pressure delivered via a sleeve. Failure occurs by shear at a steep angle through the core. If the core is drilled perpendicular to the bedding planes or other foliation then shear is across these. This may not represent the failure situation in the rock mass, where failure may be at some other orientation.

Triaxial Elastic (E_i, V_{ij}, α_i)

This test is designed to enable the measurement of the elastic parameters of rock. It involves fitting a section of core with three strain gauge rosettes and putting it in a triaxial cell. The core is sequentially loaded with incremental axial and confining loads while the strains are monitored. The Young's moduli and Poisson's ratios of the rock are derived on the basis that the rock behaves in an orthotropic manner, with one principal axis coincident with that of the core. This requires some assumptions about the behaviour of Poisson's ratio (Gray, Zhao and Liu, 2018).

If gas injection is incorporated into the test procedure the poroelastic behaviour of the rock can be determined. The poroelastic coefficients (α_i) describe the deformation of the rock brought about by fluid pressure changes. Unlike the scalar Biot's coefficient usually used for poroelasticity, the values derived from this test process are tensors related to direction.

In most sedimentary rock the Young's moduli, Poisson's ratios and poroelastic coefficients are quite nonlinear, and the results are presented as isopach plots of their tangential value versus axial and confining stress. A typical test involves in excess of 100 individual stress states.

Hydrostatic Testing (E_i)

This test is used to determine the relative stiffness of rock fragments or core in three axes. The test involves fitting the rock sample with three strain gauge rosettes. It is then cast in silicone and is hydrostatically loaded.

The analysis is based on the assumption that one of these axes is in the direction of a principal value of Young's modulus and that the core behaves in an orthotropic manner. The analysis cannot on its own be used to determine absolute values of Young's moduli and Poisson's ratios, as these cannot be separated. If a value of Poisson's ratio can be estimated then the values of Young's moduli can be calculated. Where the hydrostatic test is used in combination with uniaxial testing, so that the value of the Axial Young's modulus is measured, the other moduli and the values of Poisson's ratios can be determined. Where the core is non-linear or exhibits high Poisson's ratios, the analysis becomes complex.

The test method is particularly useful to evaluate the moduli of rock fragments or odd shaped samples such as hollow overcore samples. In the latter case the sample is also uniaxially tested.

Transverse Tensile Testing

This test is a measure of the tensile strength of a biscuit shaped sample of rock core. In this the width of the specimen is approximately ¼ the core diameter. It involves gluing two pairs of plates to each side of the core section. The core is then loaded to break the rock in tension while monitoring the deformation across the gap between the plates prior to failure. This enables a tensile modulus to also be measured and any uneven loading to be detected.

The test is particularly relevant to tensile failure perpendicular to bedding or foliation and has particular applicability in determining goaf formation characteristics.

Axial Tensile Testing

This test is used to measure the tensile strength of core to axial loading. It follows ASTM D2936-20. It involves gluing tubes to each end of a piece of core and then axially loading it to failure. The results are reported in terms of tensile stress.

In homogeneous rock the result of the test is a simple tensile strength. If conducted on core which is laminated perpendicularly to the core it provides the tensile strength across the laminations. This may be particularly relevant to roof falls or caving behaviour in laminated rock.

Slake Testing

Slake Durability is assessed by the Emerson crumb test (ECT). This is a simple test conducted on rock fragments to see whether they are susceptible to disassociation in water. The test is aimed at determining whether the roof or floor of the mining section will react to water and break up. The test classifies the rock behaviour when immersed, based on particle coherence and dispersion in water. Rocks are divided into seven classes based on their coherence in water.

Point Load Strength Index Testing

Point load testing involves loading a piece of rock with a 5 mm radius hardened steel point to induce breakage. The loading induces compression at the point of contact, with possible compressive failure below it. It also induces tensile stress in the rock perpendicular to the compressive loading. The combination of these stresses leads to failure. The failure involves splitting that includes compressive, tensile and shear components.

While the test may be used on irregular rock specimens it is frequently used on core. The value of point load is corrected for different size lumps or core. When used in this manner it is common to test pieces of core under axial load as well as across the core diameter. This provides a direct comparison of the strength in each loading direction. When loading is in the direction of laminations, the test specimen will tend to split on these.

Generally three tests in each direction are used, and the mid value is used to arrive at an I_{S50} value which represents the index normalised to a 50 mm size specimen. The test is readily used in the field as part of core logging.

ASTM D5731-07 shows a correlation between uniaxial compressive strength and the point load strength index value.

Brazilian Test

The Brazilian test involves loading a section of core placed between platens to failure. The loading is across the diameter of the core and induces tensile stress perpendicular to the loading. The loaded core fails under a combination of compression and tension. The result is generally quoted in terms of tensile stress. If the core used is drilled perpendicular to bedding or foliation, the split induced by the test will be perpendicular to this. The test does not do the same job as true tensile or point load testing.

Sigra has field operational Brazilian test equipment, but prefers to use the true tensile tests conducted in the laboratory to obtain precise numbers.

Protodyakanov Index Test (f)

This is a very simple and useful test that involves dropping a weight contained in a tube repeatedly on to fragments of rock and measuring the resultant reduction in size of these. The test is used extensively in Russian strength description of rocks. It provides an immediate basis for understanding the strength of these. The test can be conducted in the field.

Other Tests

A number of the tests presented here have been developed by Sigra because there were no suitable tests. These include the Cyclic Uniaxial, Simple Shear, Triaxial Elastic, Hydrostatic and Transverse Tensile tests. Other test processes have been modified to suit the rock type, notably the GOST Shear test which is modified to shear across bedding planes of sedimentary material.

Sigra can develop other tests to suit needs. One that we have developed but is infrequently used is to measure creep in potash cores at temperature.

CYCLIC UNIAXIAL TESTING WITH STRAIN MEASUREMENT

Typically a core sample is taken which preferably has a length that is more than 2.5 times the diameter. The ends are ground flat and parallel. However, if for example there is even a 0.1 mm difference in length along the sides of a 150 mm long core this corresponds to a strain difference of 667 microstrain before the ends are in full contact with the platens of the test machine. If the sample has a Young's modulus of 5 GPa this approximately corresponds to a stress on one side of the sample end of 3.3 MPa while the other side is not loaded. The uneven stress generated by such uneven loading becomes greater with increasing modulus. It is very easy to break a sample by applying uneven loading. Even if breakage does not occur the problem exists of measuring a core stress strain behaviour with uneven strains.
To avoid this uneven loading, due to misalignment, one end of the specimen is usually loaded through a spherical platen arrangement.

The uniaxial testing involves attaching three axial and three circumferential strain rosettes to the core sample. It is then loaded into a universal test machine for uniaxial loading. The position of the spherical end platen is adjusted to remove uneven loading and a loading test is performed.

An example of a uniaxial test specimen ready for testing is shown in Figure 2. If the test only involves loading then this can be performed at a constant deformation rate until failure is observed. This type of test does not enable the elastic component of deformation to be separated from the inelastic and neither does it permit the unloading characteristics to be determined. To determine these, cyclic loading must be used.

Figure 2: Uniaxial test specimen fitted with axial and circumferential strain rosettes

A typical approach to cyclic loading is to estimate the uniaxial strength of the sample and to plan to load it in cycles, each of which increases the loading by 10% of the estimated failure load. Our procedure is then to pick the stress and strain values at the start, peak load and after unloading. The pick from start of loading to the peak load for the cycle can be used to provide a secant loading modulus for the peak stress level in question. If the sample is then unloaded the difference in picks from the peak load situation and the unloaded situation can be used to determine the unloading secant modulus. The values of Poisson's ratio may be determined similarly. Figure 3 shows a typical cyclic loading sequence with time. Figure 4 shows this loading as a plot of stress (y axis) versus axial strain (x axis, RHS) and circumferential strain (x axis, LHS).

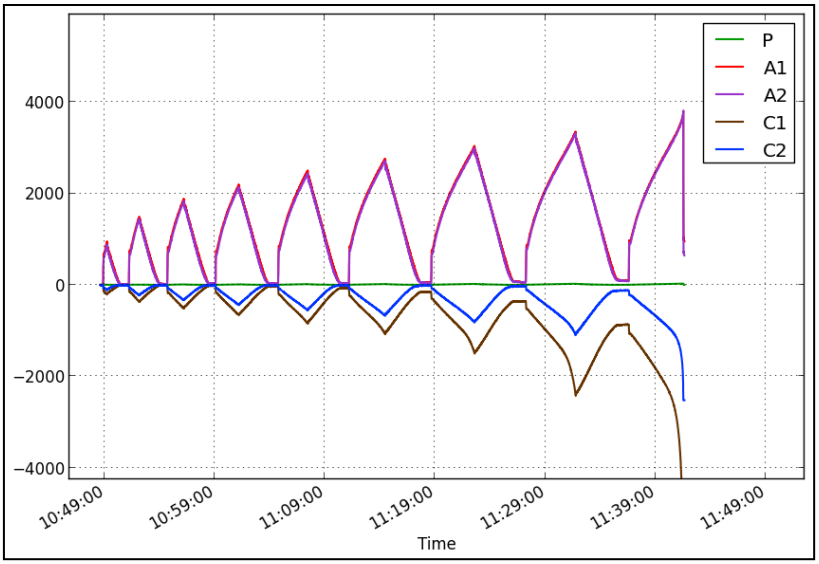

Figure 3: Axial and circumferential strains versus time

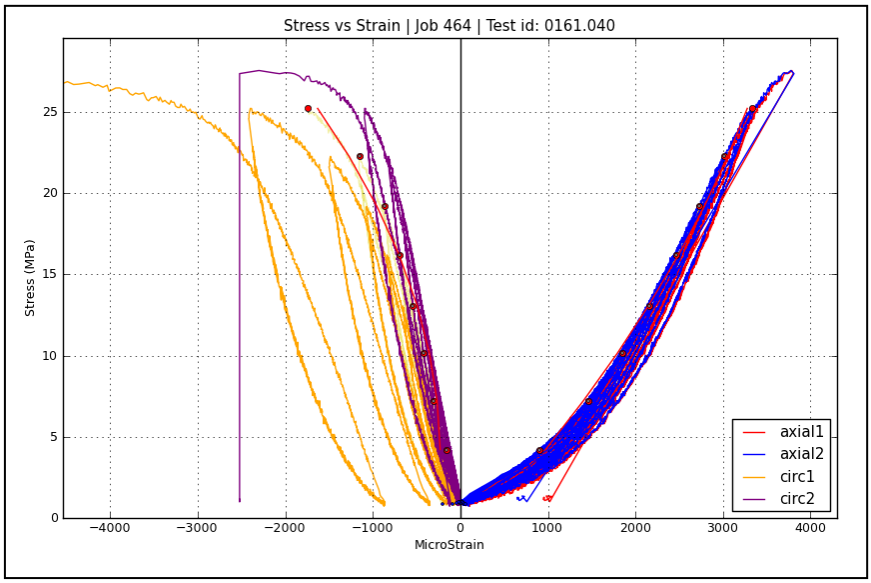

Figure 4: Plot of axial and circumferential strains versus axial stress for a sandstone

In analysing a uniaxial test it is useful to pick the strains at the start of the loading cycle, the peak load and at the end of the loading cycle. These picks are shown schematically in Figure 5. Here the axial strains are shown to the right and the circumferential strains are shown to the left. In this it can be seen that the slope of the secant drawn between points A and B

represents the loading secant modulus as does the slope between points C and D. The slope of the straight line between points B and C represents the unloading secant modulus. The permanent offset from the full loading cycle A-B-C is the difference in strain between points A and C. The circumferential behaviour may be analysed similarly.

The concept of a form of circumferential modulus, *A*, is useful here. *A* is the slope of the axial stress versus circumferential deformation. The secant loading value of *A* in Figure 5 are the slopes of the line A-1 and 2-3. The unloading secant value of *A* is the slope of the line 1-2 while the tangent value of *A* is the slope of the line 1-3.

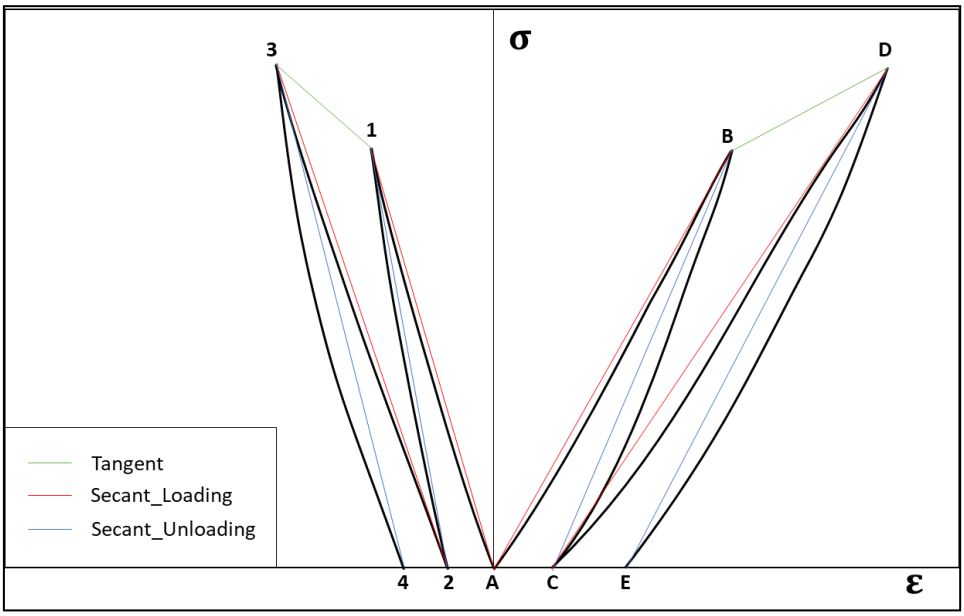

Figure 5: Picks of load and strains from a uniaxial test – schematic

Permanent deformation of the sample is an important parameter in understanding how a rock behaves. It is a useful practice to plot the total residual deformation at the end of a loading cycle versus the peak stress value achieved in the previous loading cycle. This gives a direct indication of how the sample is deforming permanently. Figure 6 shows the permanent deformation following a loading cycle. This shows that while the residual circumferential strain is initially lower than the residual axial strain this ceases to be the case once the loading has reached 15 MPa. This form of permanent deformation is quite characteristic of weaker sedimentary rock.

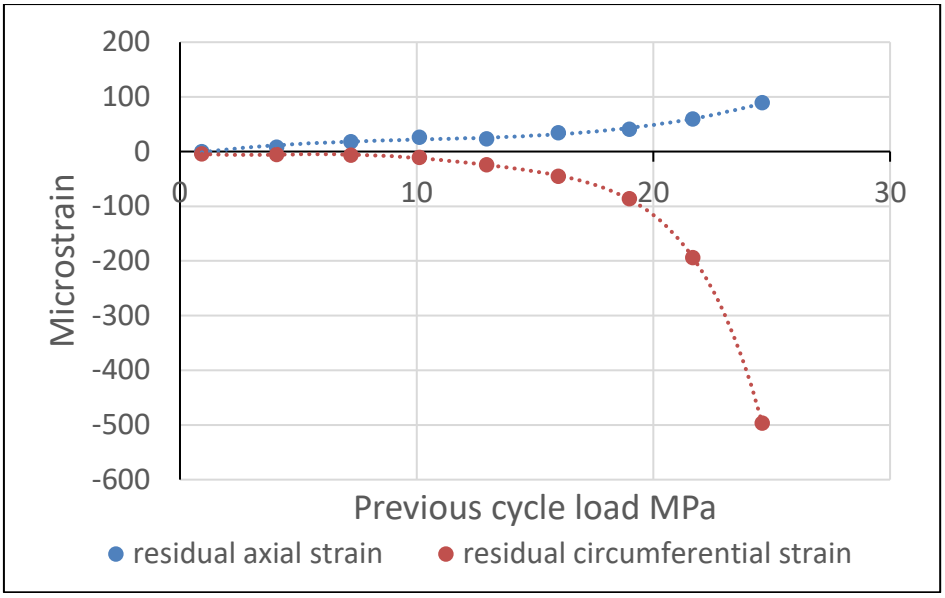

Figure 6: Residual strains following loading

There are multiple ways to determine Young's modulus and Poisson's ratio of a uniaxial test. These may be secant or tangent values and can either be corrected for the effects of permanent deformation or not. The options also exist to look at tangent values on the basis of incremental change in stress and strain or based upon the end loads of cyclic testing.

The tangent modulus can be determined by examining the incremental changes in load and deformation. Doing this does not however allow for any separation of permanent deformation from the elastic component. The results may also tend to be noisy, depending on the time interval of measurement and how much filtering is applied to the data. Different loading cycles may have different shapes. The result tends to be a cloud of information on the Young's modulus and Poisson's ratio for a sample. A good result of such an approach used to analyse a cyclic uniaxial test is shown in Figure 7.

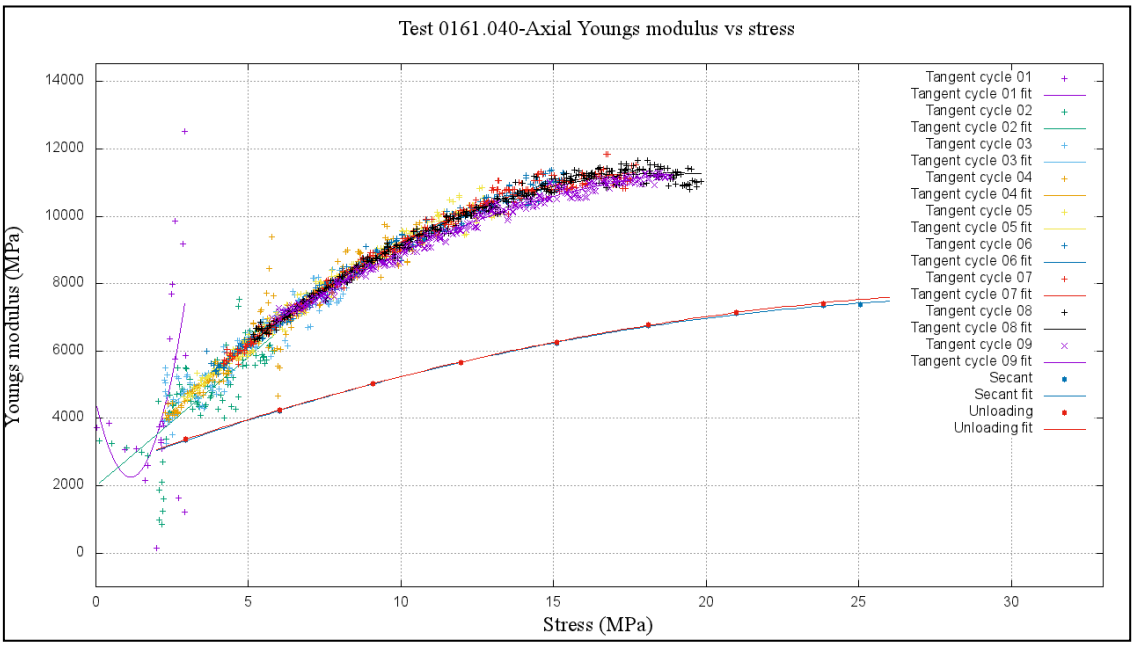

Figure 7: Tangent loading Young's modulus calculated by data points

It is possible to reduce the amount of data to be handled by examining the end points of loading and unloading. It is also readily straightforward to separate the effects of elastic deformation from permanent deformation. This can be done by simply subtracting the permanent deformation at the end of each loading cycle in the calculation of a mean secant modulus. Doing this for the cases of loading shown in Figure 5 leads to Equation 1.

$$E_{sae} = \frac{2\sigma_B - \sigma_A - \sigma_C}{2(\varepsilon_B - \varepsilon_{C)}} \quad (1)$$

Where E_{sae} is the mean axial secant modulus evaluated at stress σ_B with the effect of permanent deformation having been removed. All the strains used in Equation 1 are axial strains.

By a similar procedure it is possible to arrive at a similar equation for the secant circumferential modulus, *A*. This is shown in Equation 2.

$$A_{sae} = \frac{2\sigma_B - \sigma_A - \sigma_c}{2(\varepsilon_1 - \varepsilon_{2)}} \quad (2)$$

There is a direct mathematical relationship between the secant modulus and the tangent modulus. This is developed in section below, ***Relationship between tangent and secant Young's moduli and Poisson's ratios from uniaxial testing*** and summarised in Equation 3.

$$E_{Ta} = \frac{d}{d\varepsilon}(E_S)_a + E_{Sa} \quad (3)$$

Where E_{Ta} is the tangent modulus at point *a*

$\frac{d}{d\varepsilon}(E_S)_a$ is the derivative of the secant modulus with respect to strain evaluated at point *a*

E_{Sa} is the secant modulus evaluated at point *a*

An equation of the same form as Equation 3 can also be applied to develop a tangent circumferential modulus. Figure 8 is derived from Figure 4. It shows the mean stress and strain endpoints for the axial and circumferential strain versus stress.

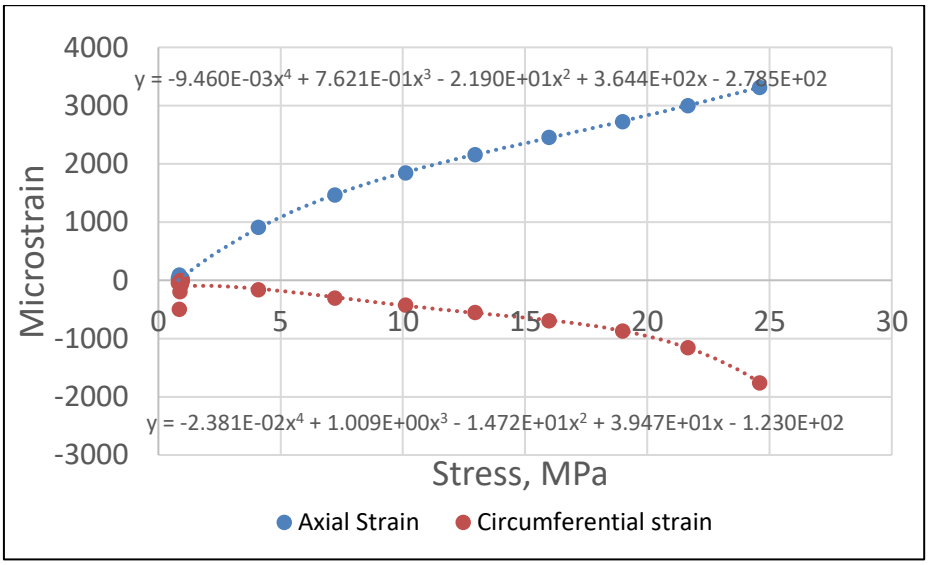

Figure 8: Endpoints of stress and strains from cyclic loading cases

Using the data presented in Figure 8 we can now calculate the following forms of Young's modulus.

1) The direct secant loading modulus without correction for permanent offset
2) The direct secant unloading modulus without correction for permanent offset
3) The average secant modulus with correction for permanent offset
4) The tangent modulus as per Equation 3 with a correction for permanent offset
5) The direct tangent modulus without correction for permanent offset

These are presented in Figure 9. The legend is in the same order as the cases above. As can be seen the secant Young's moduli for loading, unloading and mean (corrected for permanent offset) cases are almost identical. The tangent moduli are similar until the higher stresses when permanent offset makes the one derived with a correction for permanent offset a bit higher in value. The tangent moduli are significantly different from the secant ones. This is a function of the non-linearity of the sample behaviour.

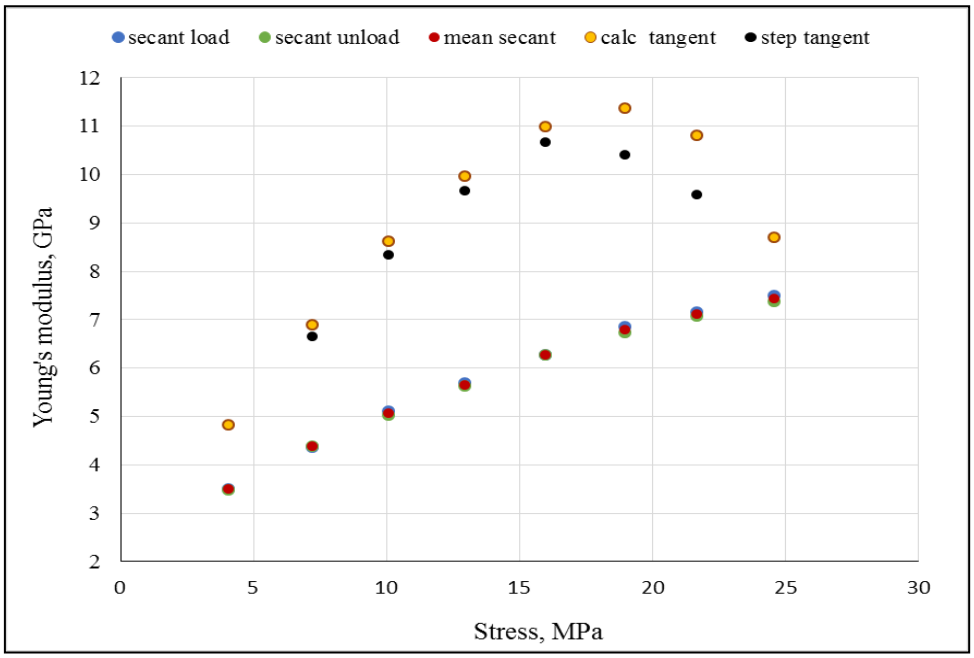

Figure 9: Plots of Young's moduli versus stress derived from the same uniaxial test

If we calculate Poisson's ratio as the negative ratio of the Young's modulus divided by the circumferential modulus, *A*, in the different forms then we get the following cases.

1) The direct loading secant value of Poisson's ratio without correction for permanent offset.
2) The direct unloading secant value of Poisson's ratio without correction for permanent offset.
3) The mean secant value of Poisson's ratio with correction for permanent offset.
4) The calculated value of tangent Poisson's ratio with correction for permanent offset.
5) The direct tangent value of Poisson's ratio without correction for permanent offset.

These are shown in Figure 10 with the legend being in the same order as the cases above.

There is a small difference between the loading and unloading secant cases. This becomes more pronounced at higher stresses when offset strains get higher. The mean secant modulus is very

close to the unloading secant case. The calculated tangent is based on the approach of Equation 3 using data corrected to remove permanent offset. The case of real note is that of the simple tangent values of Poisson's ratio with no correction for permanent offset. These increase rapidly with stress as the permanent offset component of their value becomes greater. When calculated in this form the tangent Poisson's ratio becomes more of an indicator of permanent offset, and hence the approach of failure, than anything else.

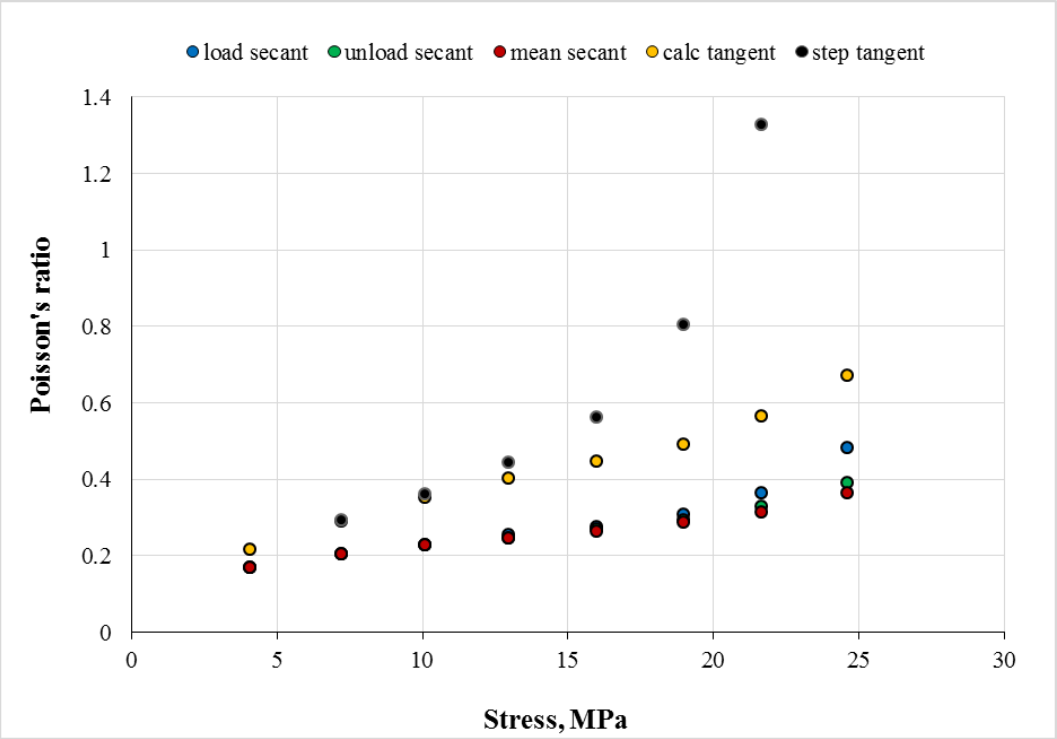

Figure 10: Poisson's ratios calculated by various methods

Uniaxial test rock properties are normally reported at half the failure stress. In this case the secant Young's modulus and Poisson's ratio would normally be reported as 5.4 GPa and 0.25. In reality the range of the secant Young's modulus is 2.5 to 7.4 GPa while that for the secant Poisson's ratio is 0.15 to 0.48.

In the case of the tangent properties the reported Young's modulus would be 9.5 GPa compared to a range of 2.5 to 11.4, depending on the method of calculation. The value of Poisson's ratio that would be reported is 0.44 whereas if it were to be calculated properly it could lie somewhere between 0.5 and 0.33. These are very big differences and it is necessary to look at the data and to ask how the values are arrived at. Also, most importantly, the question should be asked as to what it means in the context of the rock mechanics problem being considered? It is certainly not possible to say that most sedimentary rock has a specific value of modulus. Frequently it is not possible to get a sensible value of Poisson's ratio out of a uniaxial test and recourse should be made to a triaxial test, as quite a small degree of confinement can dramatically reduce the apparent value of Poisson's ratio.

The cases presented in Figure 3 to Figure 10 are for a medium grained sandstone which is quite nonlinear and exhibits some permanent offset. It is however quite testable. Figure 11 presents a typical stress – strain plot for coal. It is nonlinear, exhibits huge permanent offset and starts to fail at a very low stress because of lack of confinement. This plot exemplifies the difficulties in uniaxial testing of coals, and for that matter weaker rocks, in the hope that it is

possible to get sensible values of Young's modulus and Poisson's ratio. Frequently the only piece of coal that can be tested is totally unrepresentative of the rest of the coal seam.

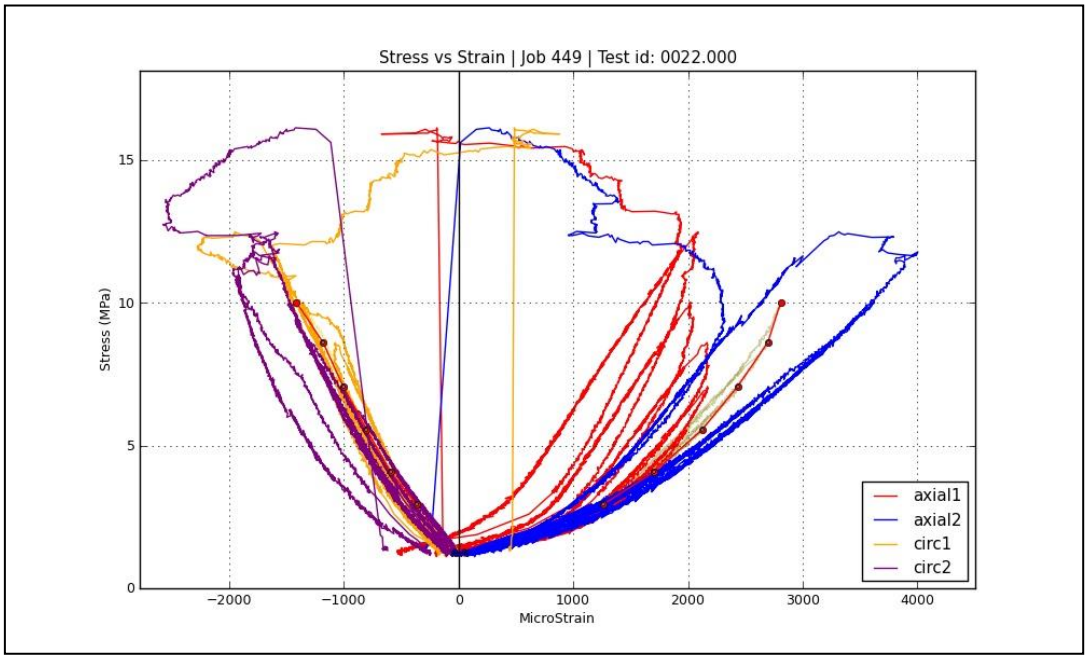

Figure 11: Plot of axial and circumferential strains versus axial stress for a typical coal sample

Relationship between tangent and secant Young's moduli and Poisson's ratios from uniaxial testing

The tangent axial Young's modulus is defined by Equation 4.

$$E_{T1} = \frac{d\sigma_1}{d\varepsilon_1} \tag{4}$$

The secant axial Young's modulus is defined at some point *a* on the loading or unloading curve as Equation 5.

$$E_{S1a} = \frac{\sigma_{1a}}{\varepsilon_{1a}} \tag{5}$$

This can be alternatively described in Equation 6.

$$E_{S1a} = \int_0^{\varepsilon_{1a}} \frac{d\sigma_1}{d\varepsilon_1} d\varepsilon_1 / \varepsilon_{1a} \tag{6}$$

Which may be rewritten as Equation 7.

$$E_{S1a} = \int_0^{\varepsilon_{1a}} E_{T1} d\varepsilon_1 / \varepsilon_{1a} \tag{7}$$

By re-arranging Equation 7 to Equation 8.

$$\int_0^{\varepsilon_{1a}} E_{T1} d\varepsilon_1 = E_{S1a}\varepsilon_{1a} \tag{8}$$

By differentiating Equation 8 with respect to strain we get Equation 9.

$$E_{T1a} = \frac{d}{d\varepsilon_1}(E_{S1a}).\varepsilon_{1a} + E_{S1a}.\frac{d}{d\varepsilon_1}(\varepsilon_{1a}) \tag{9}$$

Re-arranging we get Equation 10

$$E_{T1a} = \frac{d}{d\varepsilon_1}(E_{S1a}).\varepsilon_{1a} + E_{S1a} \tag{10}$$

Where E_{T1a} is the tangent Young's modulus in the axial (1) direction at strain ε_{1a}
E_{S1a} is the secant Young's modulus in the axial (1) direction at strain ε_{1a}

Equation 10 describes the Tangent axial modulus in terms of the secant axial Young's modulus, its derivative with respect to strain and the axial strain at which it is being evaluated. Because the secant Young's modulus is being used the effect of an offset strain is minimised because it is spread over the entire loading strain.

Let us define a modulus type term, *A*, relating axial stress and lateral strain associated with axial stress in Equation 11.

$$A_{T2} = \frac{d\sigma_1}{d\varepsilon_2} \tag{11}$$

Then it is possible to follow identical steps as for the axial strain case and arrive at Equation 12 which is an analogue of Equation 10 only defined in terms of circumferential strain.

$$A_{T2b} = \frac{d}{d\varepsilon_2}(A_{S2b}).\varepsilon_{2b} + A_{S2b} \tag{12}$$

Where A_{T2b} is the tangent value of axial stress with respect to circumferential strain at strain level b

A_{S2b} is the secant value of the axial stress with respect to circumferential strain at strain level b

The tangent value of Poisson's ratio is defined in Equation 13 in which the values of the tangent Young's modulus and the tangent value of A are evaluated at the same axial stress level.

$$v_{T12} = -\frac{d\varepsilon_2}{d\varepsilon_1} = -\frac{\frac{d\sigma_1}{d\varepsilon_1}}{\frac{d\sigma_1}{d\varepsilon_2}} = -\frac{E_{T1a}}{A_{T2b}} \tag{13}$$

The secant Poisson's ratio is simply the negative ratio of the circumferential to axial strain associated with total loading or unloading as in Equation 14.

$$v_{S12} = -\frac{\varepsilon_2}{\varepsilon_1} \tag{14}$$

The process to determine the tangent axial Young's modulus and the tangent Poisson's ratio is as follows.

1) Cyclically load the sample
2) Plot the load and strain data on a time base.
3) Pick the load and strain for the initial unloaded case.
4) Pick the load and strain for the full load case
5) Repeat 3 & 4 until the end of the test. This is usually the sample failure
6) Calculate the unloading cases of the secant Young's modulus E_{S1} for each load cycle
7) Calculate the unloading cases of the secant value of A_{S2} for each load cycle
8) Plot the values of the unloading E_{S1} and A_{S2} for each cycle
9) Fit a simple differentiable function to each of the cases being considered. This could be a linear equation, a more complex polynomial or a cubic spline
10) Solve Equation 10 for the tangential Young's modulus E_{T1}
11) Solve Equation 12 for the tangential value of A_{T2}
12) Solve Equation 13 for the tangential Poisson's ratio

SIMPLE SHEAR TESTING

The core shear strength testing procedure involves placing the core sample into the testing saddle that is resting on the bottom loading platen of the universal test machine.
The top section of the shear testing apparatus is placed on top of the middle section of the core resting on the lower saddle.

The sample is then loaded in compression by the universal test machine until shear failure occurs with the load at failure recorded. Frequently, the core sample can be moved sideways and sheared again.

To calculate the shear strength, the core diameter of the sheared face is recorded and used to determine the shear surface area.

Generally, one side of the core section shears before the other side (depending upon which side is the weaker). Consequently, to determine the shear strength of the core sample, half of the recorded load at failure is divided by the shear surface area to yield a shear strength

The value of shear strength determined corresponds to the value of cohesion on the failure plane.

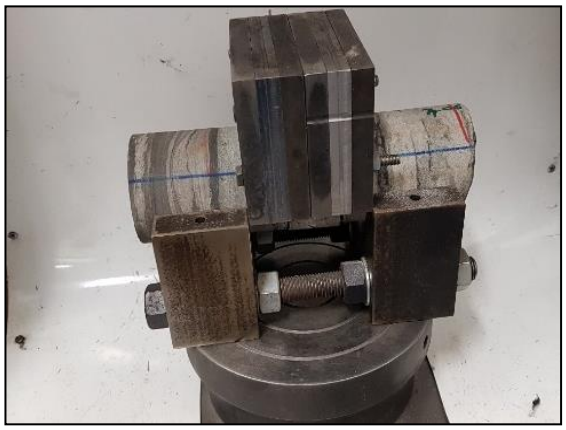

Figure 12: Direct shear test on a core specimen

Figure 13: Core Shear Strength Testing Apparatus, Top view

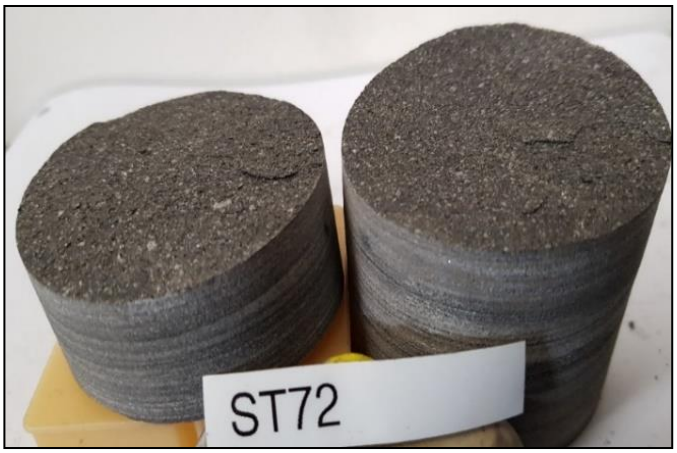

Figure 14: Test sample after failure, Side View

MODIFIED GOST (ГОСТ) SHEAR TESTING

This is a method used to determine the ultimate shear strength of core samples loaded at different angles in a universal test machine. The test apparatus is shown schematically in Figure 15 and physically in Figure 16. The results of a sheared sample are shown in Figure 17. The same sample is shown in lateral view before and after failure in Figure 18.

The loading angles (25º, 35º, 40º and 45º to the load direction) mean that different ratios of normal to shear stress are generated. The values of shear to normal stress may be directly calculated at failure and plotted as is shown in Figure 18.

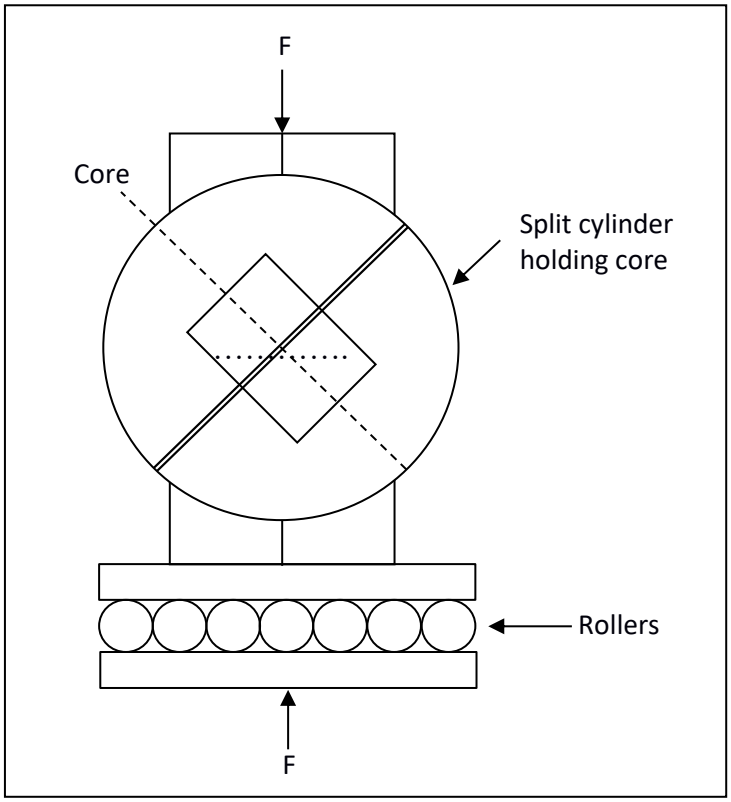

Figure 15: Modified GOST Shear Test Apparatus

Figure 16: Modified GOST Shear Test Setup

Figure 17: View of failure surface.

Figure 18: Side view of sample before and after failure.

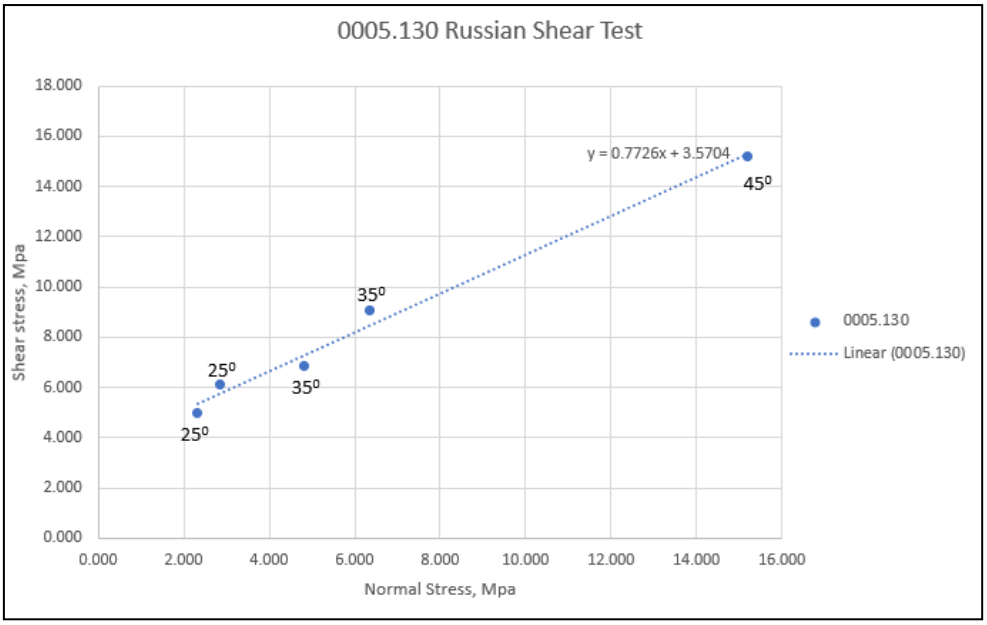

Figure 19: Modified GOST Shear Test Plot

TRIAXIAL FAILURE TEST

This test is a simple triaxial test to failure in a Hoek Cell as described in Hoek and Franklin, 1968.

TRIAXIAL ELASTIC TESTING

The triaxial testing of core involves preparing the sample of length to height ratio of greater than 2.5 The ends are ground flat and parallel. The core periphery is filled with Portland cement plaster if required to avoid strain gauge adherence or lead to squeezing of the gauge foil into pores. Three strain gauge rosettes are then adhered at 120^{o} separations around the periphery of the core. The core is then fitted into the triaxial test rig and the strain gauges are electrically coupled. A core sample is shown in this position in Figure 20. An elastomeric sleeve is then fitted over the sample and the cell is then closed ready for loading. The load is applied in a sequence of steps over a number of cycles.

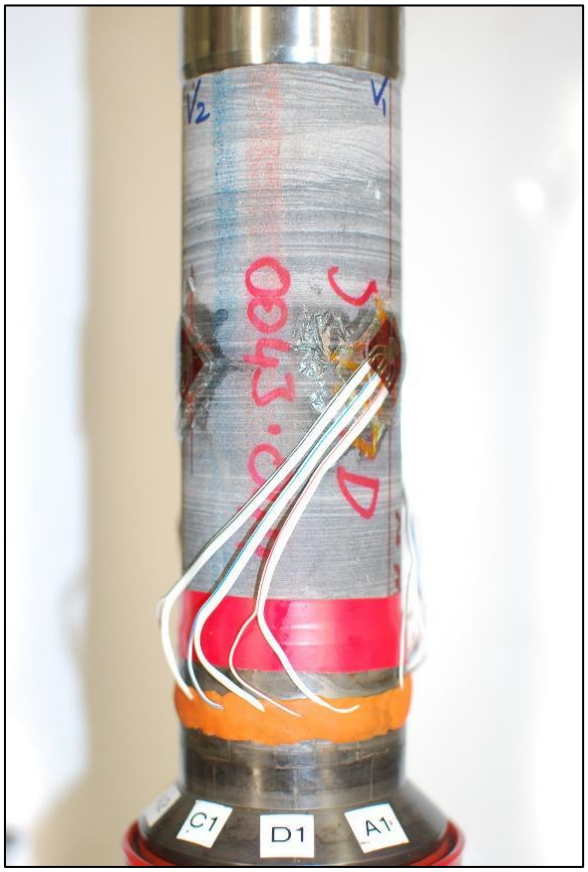

Figure 20: Showing a fine grained silty sandstone core fitted with strain gauge rosettes within the triaxial cell prior to the sleeve being fitted.

The first cycle involves a step increase in axial load followed by a step increase in radial loading to a fraction (typically 90%) of the axial load as shown in Figure 21. This process is repeated with multiple loading increments. The system is then unloaded and a second cycle is then repeated but with the radial loading fraction at a lower value (typically 75%) of the axial load change. Additional loading cycles are undertaken with reduced radial to axial loading fractions (typically 50% and 25%). Finally a uniaxial loading cycle is performed.

The reason for starting with a loading regime where the radial load is close to the axial load is to minimise the potential for shear failure to occur early in the test process. As the test cycles proceed the potential for shear failure to occur increases. The determination of poroelastic behaviour involves the pressurisation of the sample with
gas. The gas usually used is nitrogen though helium is preferable where there is a risk of adsorbing gas into the rock material. The pressure used must be less than the radial

(confining) pressure so that the gas does not cause the elastomeric sleeve to be lifted. It is also kept at as low a pressure as is compatible with obtaining a satisfactory strain reading. Sometimes the gas injection must be maintained for a significant period to ensure permeation through the sample. By monitoring the strain gauges it is possible to determine when the strain change has stopped occurring.

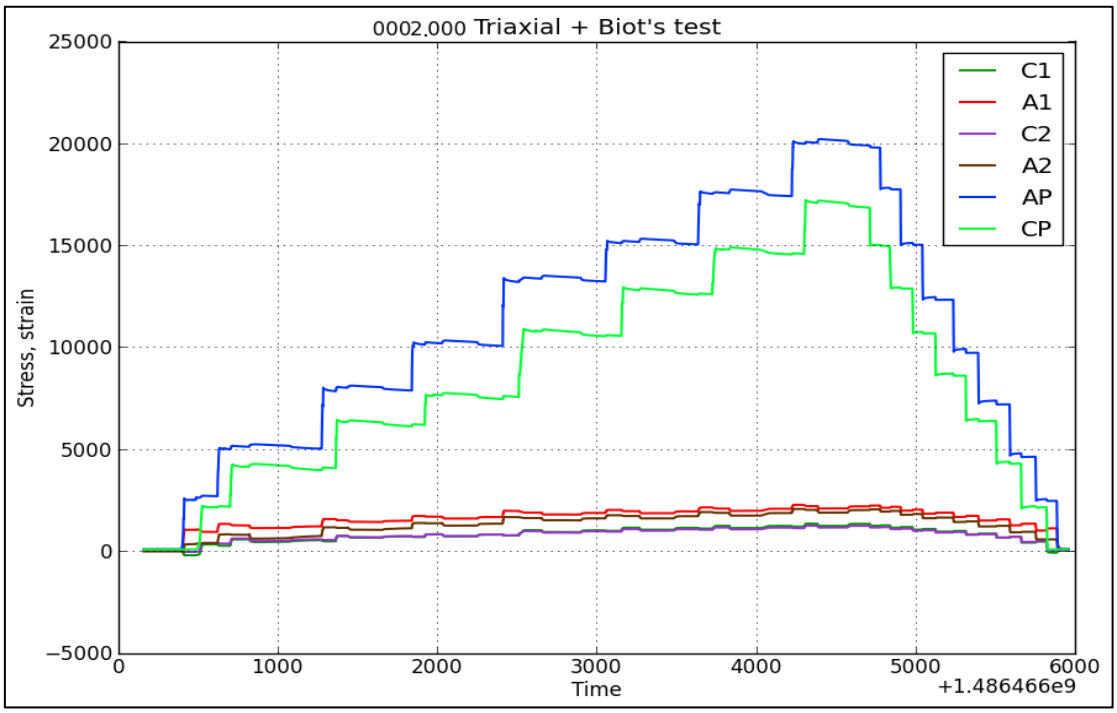

Figure 21: Example of the first cycle of stepwise axial pressure (AP) and confining pressure (CP) in kPa changes and the resulting strains in microstrain.

The analysis of the tests are on the basis of the rock behaving as an orthotropic solid. This presented in Gray, Zhao and Liu (2018). The results of it are presented in terms of isopachs of tangent Young's moduli in each direction and in terms of the six associated values of Poisson's ratio. The Poisson's ratios associated with axial loading are directly measured while those associated with transverse loading utilise the assumption that a geometric mean Poisson's ratio exists which is described in Equation 15.

$$\boldsymbol{v_a = \sqrt{v_{ij} v j i}} \qquad (15)$$

The poroelastic behaviour is presented as a tensor rather than the more common scalar Biot's coefficient.

An example of plot of axial Young's modulus (E_1) for a porous sandstone is given in Figure 22.

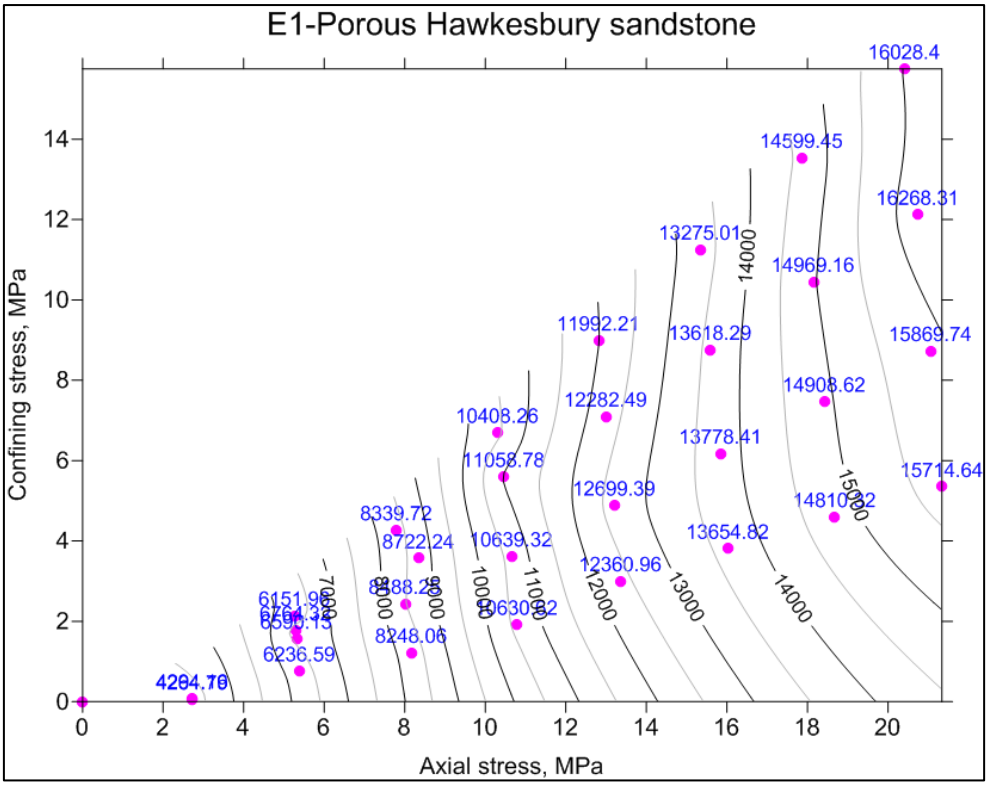

Figure 22: Axial Young's modulus for a core of porous sandstone drilled perpendicular to the bedding.

HYDROSTATIC TESTING

It is frequently impossible to obtain a suitable sample of a rock to be tested triaxially, and testing must be undertaken on a fragment or in the case of an overcore for stress measurement purposes a hollow core sample.

The sample is fitted with strain gauge rosettes. It is convenient to orient these so that they either match any particular direction of anisotropy that can be observed or are oriented with the core. Once the gauges are fitted the sample is then cast in an elastomeric resin which is then allowed to set. Figure 23 shows such a sample. The strain gauge leads are then connected and the sample is sealed in a vessel which is fluid filled and pressurised in a series of pressure steps. Because the resin used is very much less stiff than the rock sample, the hydrostatic load is directly transferred to the rock surface.

Figure 23: Strain gauged phyllite sample cast in silicone resin.

Because the loading is hydrostatic it is impossible to separate Poisson's ratios from Young's moduli in the analysis. To solve for Young's moduli and general Poisson's ratios it is necessary to assume something. This can be a geometric mean value Poisson's ratio or a value of Young's modulus. The latter is more generally used when the method is used for overcoring. In this case a hydrostatic test is undertaken with on the overcore and then the overcore is uniaxially loaded to get the axial Young's modulus. If this is linearly elastic the solution is straightforward but if it is nonlinear it is not. Gray, Zhao and Liu (2018) describe the analysis in more detail.

TRANSVERSE TENSILE TESTING

In many cases the prime means of failure in a rock mass is tensile. Examples of this are caving zones including the goaf edge of a longwall. The most commonly used method to measure tensile strength is the Brazilian test (Ulusay, R. and Hudson, H.A, 2007). This is in fact a compressive test across the diameter of the core and failure is partly by tension, induced by the geometry of loading, and partly by shear. Its analysis for tensile strength is also dependent on the core behaving in a linearly elastic manner. The test tends to predict a tensile strength value that is high.

It is possible to undertake true tensile testing of rock. The complication of how to hold on to a piece of rock in tension is fairly easily resolved by the use of high strength epoxy glues in shear. Tensile loading may be applied easily along the axis of the core and equally so transversely to the core. In the latter case, the core is cut transversely to form a biscuit of rock which is normally a quarter of the diameter (15 mm for HQ-3 sized core) as is shown in Figure 24.

This core is then glued between two steel plates on each side of the biscuit leaving a gap of one eighth the core diameter (8 mm for HQ-3 core) in between as shown in Figure 25. The sample is fitted into a universal test machine and the gap is monitored on each side by strain gauged C rings as is shown in Figure 26. The core biscuit is then loaded via these plates using a load balancing system side plate and the load versus deformation value determined.

Almost invariably one side of the core biscuit fails before the other due either to inhomogeneity in the rock or due to uneven loading leading to some degree of bending in the sample. The latter may be corrected by analysis of the uneven deformation of each side of the core to arrive at a more accurate tensile strength.

Figure 24: Prepared sample disc

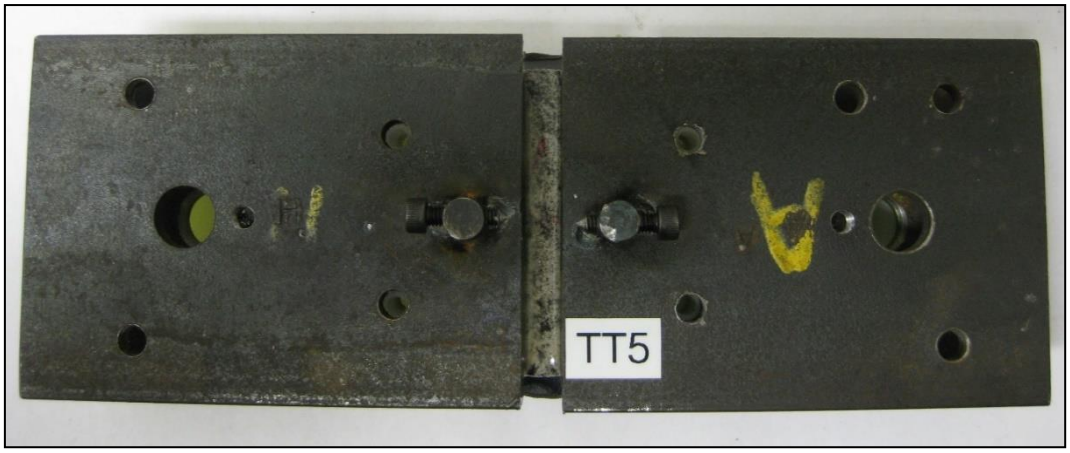

Figure 25: Prepared sample glued between two sets of steel plates.

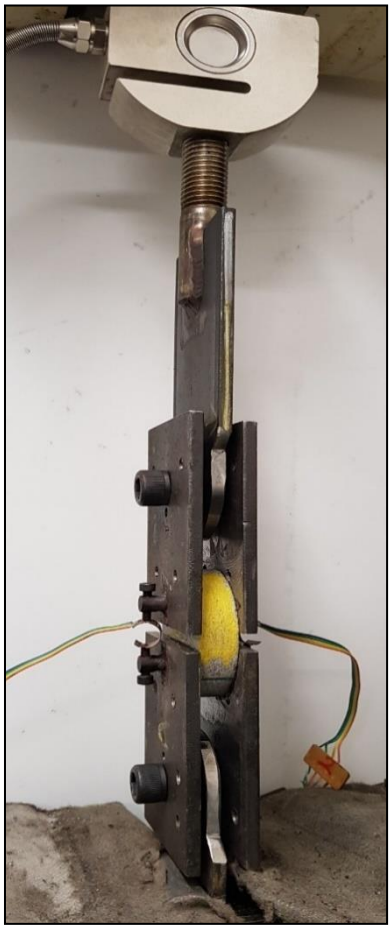

Figure 26: Test sample before in UTM before failure

Figure 27: Failed transverse tensile test disc.

To calculate the transverse tensile strength, the width and depth of the failed face is recorded and used to determine the failure surface area.

To determine the transverse tensile strength (taking into account any uneven loading) of the core sample, the increasing applied stress is plotted against the recorded strains. The strains are averaged and the established point of failure plotted against the averaged strain value to yield a corrected transverse tensile strength value. This is shown in Figure 28.

The deformation measurement via the strain gauged C rings enables an estimation of the tensile modulus value of the core.

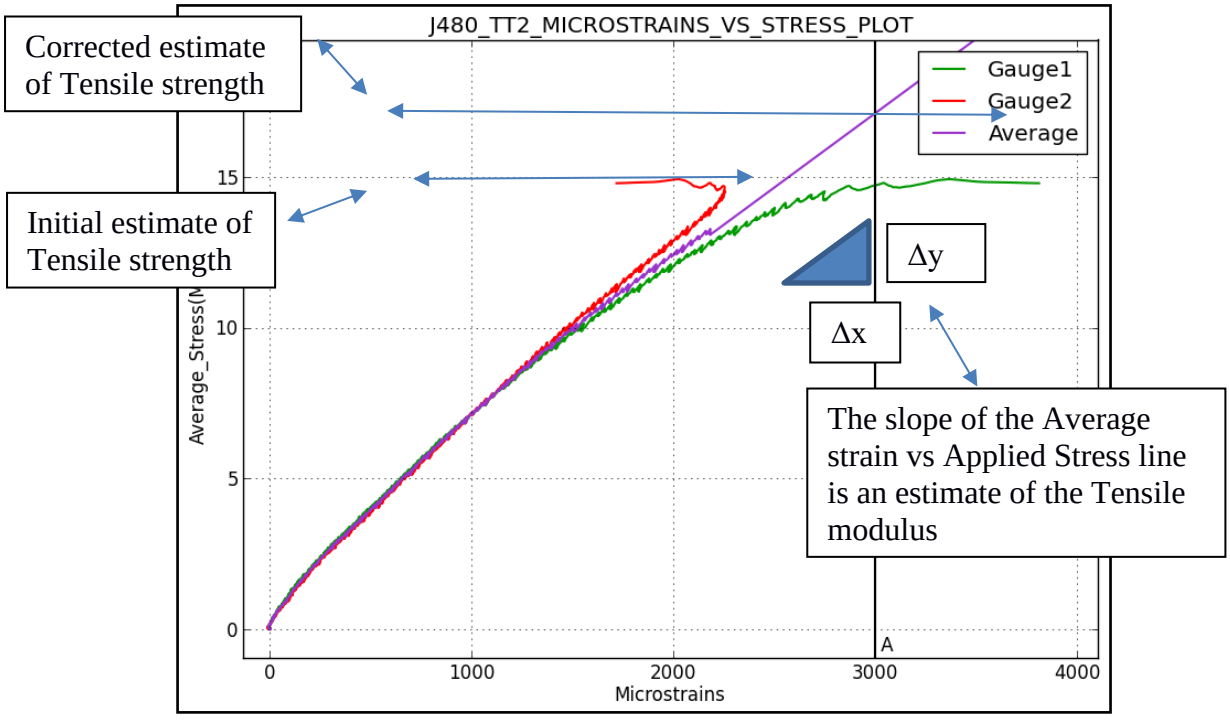

Figure 28: Example Plot of Microstrain vs Applied Stress

AXIAL TENSILE TESTING

The test is performed to measure the axial tensile strength of a rock specimen (ASTM D2936-20), especially in order to the determine the strength of a weak bedding plane.

The axial tensile strength testing involves cutting the core sample to approximately 80mm length, gluing it into split cylindrical tube ends leaving approximately 25mm of core exposed in the middle.

The sample is then placed into the universal test machine and loaded in tension until failure occurs with the tensile load at failure being recorded.

Figure 29: Example of Axial Tensile Test

Figure 30: Tensile test specimen before and after testing.

SLAKE TESTING

This test classifies the behaviour of rock, when immersed, based on particle coherence and clay dispersion in water. Testing is done only on relatively soft rocks or soils with suitable aggregates. Competent rock, sands and gravels are usually unsuitable for the test.

This method describes the procedure for the determination of the Emerson Dispersion class number of a rock. Rocks are divided into seven classes on the basis of their coherence in water. The rock specimen will be collected, tested and assessed according the assessment of rock behaviour in Figure 31.

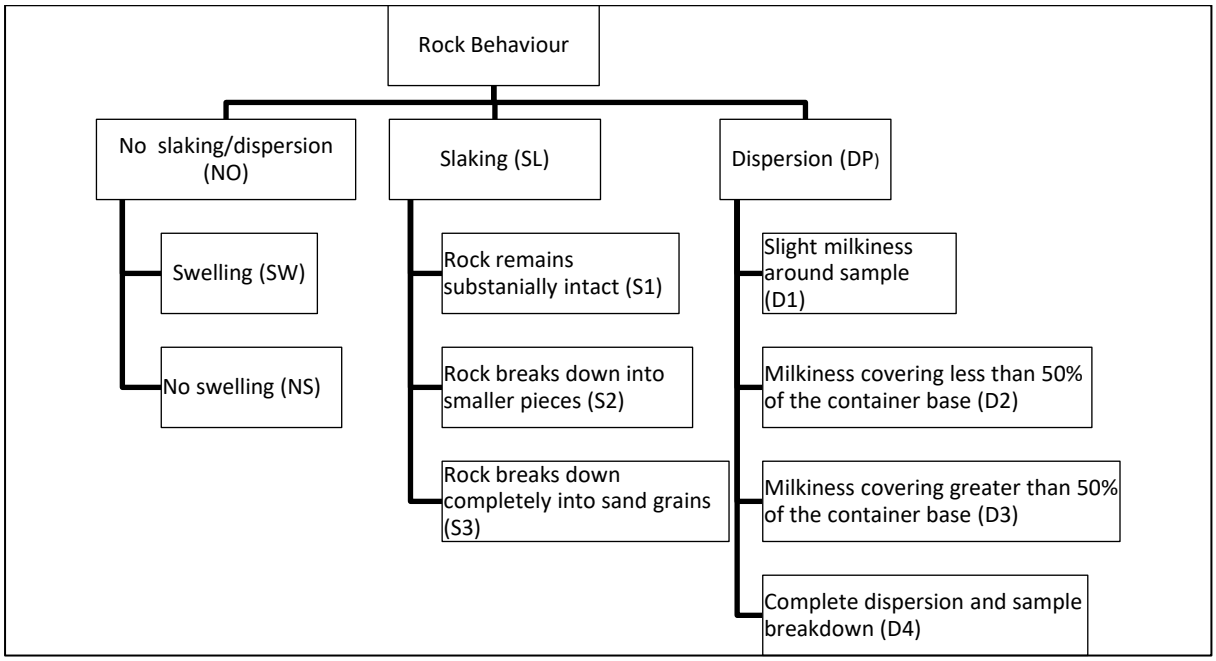

Figure 31: Assessment of Rock Behaviour

POINT LOAD STRENGTH INDEX TESTING

The test is used as an index test for the strength classification of rock materials. It can be used to predict the uniaxial tensile and compressive strength. The Point Load Strength Index ($I_{s(50)}$) and the Strength Anisotropy Index ($I_{a(50)}$) can also be measured by the Point Load Test.

Little or no specimen preparation is need. The rock specimen can be the core (diametral and axial tests), cut blocks (the block test) or irregular lumps (the irregular lump test). The concentrated load is applied to the rock specimen through a pair of spherically truncated, conical platens.

The point load test (ASTM D5731-07) is another useful test for strength and mode of failure. The point load test involves loading a piece of rock between two points with a radius of 5 mm. The value of the failure load is recorded and related to the size of the specimen to arrive at a value of strength called a point load index. In anisotropic rock such as bedded sedimentary lithologies it can be used to test across, as well as along, the plane of weakness to highlight anisotropy. The point load itself induces a complex loading situation comprising compression, shear and tension. The correlation between point load and uniaxial compressive strength that is frequently used is therefore somewhat tenuous. Careful examination of the failure mode during the point load test can however reveal a lot about the strength of the rock. For example, point loading across the bedding plane, leading to shear on the bedding plane, indicates a weakness on that plane. Such a weakness should also be revealed by testing with loading parallel to the bedding plane. Point load values are corrected to that of a standard 50mm diameter core resulting in a value of $I_{s(50)}$ that is comparable across different core diameters.

Figure 32: Point load test of an irregular specimen in the laboratory.

BRAZILIAN TEST

This test is used to measure the uniaxial tensile strength of prepared rock specimen. It can be performed in the universal test machine in the laboratory or by a portable test apparatus.

The portable has been designed so the test can be performed easily on-site. The time and pressure readings during the test are be recorded by the pressure transducer inside the testing apparatus. The data can be read via an app on the mobile phone and can be sent to an email address after completing the test.

The tensile strength shall then be calculated by the following formula taken from Ulusay and Hudson, 2007 and is shown in Equation 16.

$$\sigma_t = \frac{0.636P}{Dt}(MPa) \quad (16)$$

Where P is the load at failure (N)
D is the diameter of the test specimen (mm)
T is the thickness of the test specimen measured at the centre (mm)

Figure 33: Site Brazilian test equipment – test cylinder with pressure pump

Figure 34: Test sample after failure – Side View

PROTODYAKANOV INDEX TEST (f)

The *Protodyakonov index* is measured by drop hammer test. In Russia and China it is a standard means to determine rock strength simply. It is also used to measure the proneness of a coal to fragment. It is used as part of outburst risk determination and the suitability of a seam for hydraulic mining.

This is a test on lump coal with measurement of the coal size reduction. The process involves four weighed sets of coal consisting of 5 subsamples each with size range 20 to 30 mm and weight 40-60 g. The subsample is placed in an apparatus comprising a drop hammer of 2.4 kg weight with a 600 mm travel. The diameter of the hammer is 66 mm and the tube it falls within is 76 mm. The number of hammer blows depends on coal strength and is determined experimentally. The amount of fines of less than 0.5 mm diameter is measured in a measuring cylinder (a tube of 23 mm diameter). The height of fines in the measuring tube after crushing of one set (5 subsamples) should be in the range of 20 – 100 mm, otherwise the amount of blows should be adjusted experimentally. For the coal usually one blow is enough, but for some strong coals 2-3 blows are required.

Figure 35: Drop hammer equipment – measuring cylinder with scale and tube with drop hammer.

The *f* coefficient is defined by Equation 17:

$$f_{20-30} = \frac{20 * n}{h} \tag{17}$$

Where f_{20-30} is the toughness index (for 20 to 30 mm size range)
n is the number of hammer blows

h is the scale measurement in the cylinder after 5 subsample tests (mm).
The final result is an average of 4 measurements.

The general threshold *f* value less than 0.5 is indicative of outburst proneness.

An extension to the test method for fine coal where it is not possible to obtain 20 to 30 mm lumps is to sieve the sample for the 1 to 3 mm range. This is then hammered three times and the size reduction noted by a measurement in the fines cylinder.

In this case, if $f_{1-3} > 0.25$ using equation 8.5.1 with $n = 3$

then the equivalent $f_{20-30} = 1.57 \times f_{1-3} - 0.14$;

otherwise if $f_{1-3} \leq 0.25$ then

the equivalent $f_{20-30} \equiv f_{1-3}$

References

ASTM D5731-07, 2007. Standard Test Method for Determination of the Point Load Strength Index of Rock and Application to Rock Strength Classification, ASTM International, West Conshohocken, PA.

ASTM D2936-20, 2020. Standard Test Method of Direct Tensile Strength of Intact Rock Core Specimens, ASTM International, West Conshohocken, PA.

Gray, I., Zhao, X. and Liu, L., 2018. The Determination of Anisotropic and Nonlinear Properties of Rock through Triaxial and Hydrostatic Testing, ARMS10 – The ISRM 10th Asian Rock Mechanics Symposium, ARMS10 Organizing Committee and ISRM, Singapore, 29th October 2018 – 03rd November 2018.

Hoek, E. and Franklin, J.A. 1968. A simple triaxial cell for field and laboratory testing of rock. Trans. Instn Min. Metall. 77, A22- 26

Ulusay, R. and Hudson, H.A, 2007. The Complete ISRM Suggested Methods For Rock Characterization, Testing And Monitoring: 1974-2006, ISRM Turkish National Group, Turkey, ISBN: 978-975-93675-4-1.

ГОСТ 21153.5-88. (1988). Method for the determination of rock shear strength under compression, USSR State Publisher.